

PFC/RR-82-2

DOE/ET-51013-29
UC20

Description of the Fokker-Plank Code
Used to Model ECRH of the Constance 2 Plasma

by

Michael E. Mael

January 1982
Plasma Fusion Center
Research Laboratory of Electronics
Massachusetts Institute of Technology
Cambridge, MA 02139

This work was supported by DOE Contract No. DE-AC-78ET-51013.

Description of the Fokker-Plank Code
Used to Model ECRH of the Constance 2 Plasma.

by

Michael E. Mauel

January 30, 1982

Plasma Fusion Center

Research Laboratory of Electronics

Massachusetts Institute of Technology

PFC-RR-82/2

The time-dependent Fokker-Plank code which is used to model the development of the electron velocity distribution during ECRH of the Constance 2 mirror-confined plasma is described in this report. The ECRH is modeled by the bounce-averaged quasilinear theory derived by Mauel¹. The effect of collisions are found by taking the appropriate gradients of the Rosenbluth potentials, and the electron distribution is advanced in time by using a modified alternating direction implicit (ADI) technique as explained by Killeen and Marx². The program was written in LISP to be run in the MACSYMA environment of the MACSYMA Consortium's PDP-10 computer.

This report describes both the time-dependent, partial differential equation used to describe the development of the electron distribution during ECRH of the Constance 2 mirror-confined plasma and the method by which this equation was solved. The electrons are modeled in (v, θ) phase-space, where $\theta = \sin^{-1}(v_{\parallel}/v)$. The ion distribution is considered to be a Maxwellian with known density and temperature. The ECRH is modeled with a bounce-averaged quasilinear equation which is strictly correct only for linear heating of confined particles. However, since the magnetic field is assumed to be parabolic, the heating can be "extended" into the loss cone when the potential is positive. Changes in the particle energy are assumed to occur randomly, over several passes through resonance. The potential of the plasma is also assumed to be parabolic and a known function of time. Those particles within the loss region of velocity-space are lost at a rate determined from their transit time. Each point in velocity space is advanced in time using a modified Alternating Direction Implicit (ADI) technique used by Killeen and Marx².

The report is organized into six sections. The first section describes the Fokker-Plank model for electron-electron and electron-ion collisions. The second section describes the loss-cone term from which the electron loss current is calculated. The third section describes the programming of the ECRH term. The fourth section describes the numerical method used to solve the partial-differential equation. The fifth section lists the diagnostics available to evaluate the code's performance. And, the final section gives some examples and checks of the operation of the program.

1. Collisions .

1.1. Rosenbluth Potentials . The electron-electron and electron-ion collisions are given by the Rosenbluth formulas¹, or

$$\frac{\partial F_e(v)}{\partial t} = -D_i(J_{cle}^i + J_{ion}^i) \quad (1)$$

where

$$J_\beta^i = \Gamma_\beta \left\{ F_e(v) D^i H_\beta(v) - \frac{1}{2} D_j(F_e(v) D^j D^i G_\beta(v)) \right\} \quad (2)$$

and where the potentials H_β and G_β satisfy Poisson's equation

$$\nabla^2 H_\beta(v) = -4\pi \frac{m_e}{M_{cm}} F_\beta(v) \quad (3)$$

$$\nabla^2 G_\beta(v) = 2 \frac{M_{cm}}{m_e} H_\beta(v) \quad (4)$$

and $\Gamma_\beta = 4\pi e^2 e_\beta^2 \Lambda_{e\beta} / m_e^2$. M_{cm} is the reduced mass, or $m_e m_\beta / (m_e + m_\beta)$. Note that the derivatives, D_i , in Equations 1 and 2 are covariant derivatives. This insures the obvious result that the scalar formed from the divergence of the vector J_β^i is invariant to changes in the description of the coordinate system. The integral solutions to Equation 3 and 4 are

$$G_\beta(v) = \int d^3 v' |v - v'| F_\beta(v') \quad (5)$$

$$H_\beta(v) = \left(\frac{m_e}{M_{cm}} \right) \int d^3 v' \frac{F_\beta(v')}{|v - v'|} \quad (6)$$

As will be shown in the next subsection, only $G_{cle}(v, \theta)$ need be numerically integrated. Since for each phase-space point, this integration involves a summation over all grid points and is very time consuming. Therefore, all of the coefficients for the integration is saved on disk². Equation 5 can be expressed in terms of the elliptic integral of the second kind, or

$$G_{cle}(v, \theta) = \int_0^\infty v'^2 dv' \int_0^\pi \sin \theta' d\theta' 4\sqrt{a+b} E\left(\frac{2b}{a+b}\right) F_{cle}(v', \theta') \quad (7)$$

where

$$\begin{aligned} a &= v^2 + v'^2 - 2vv' \cos \theta \cos \theta' \\ b &= 2vv' \sin \theta \sin \theta' \\ E(m) &= \int_0^{\pi/2} d\phi \sqrt{1 - m \sin^2 \phi} \end{aligned}$$

1.2. *Reduction of the Fokker-Plank Equation*. For this program, the electrons are placed in a (v, θ, ϕ, ψ) coordinate system, and Equation 1 must be expressed in terms of these coordinates. The electrons are assumed to be independent of gyrophase, ϕ , and the collision term is trivially bounce-averaged over the bounce-phase, ψ , by assuming a square-well. (The ECRH and endloss terms assume parabolic magnetic and potential profiles.)

Equation 1 becomes

$$\frac{1}{\Gamma_\beta} \frac{\partial F_e}{\partial t} \Big|_\beta = -(\partial_i F_e)(\partial^i H_\beta) - F_e \nabla^2 H_\beta + \frac{1}{2} \left\{ (D_i D_j F_e)(D^i D^j G_\beta) + 2(\partial_j F_e)(\partial^j \nabla^2 G_\beta) + F_e \nabla^2 \nabla^2 G_\beta \right\} \quad (8)$$

or

$$= -4\pi F_e F_\beta \left(1 - \frac{m_e}{M_{cm}}\right) + \frac{M_{cm}}{m_e} (\partial_i F_e)(\partial^i H_\beta) \left(1 - \frac{m_e}{M_{cm}}\right) + \frac{1}{2} (D_i D_j F_e)(D^i D^j G_\beta) \quad (9)$$

The electron and ion terms are therefore

$$\frac{1}{\Gamma_{ee}} \frac{\partial F_e}{\partial t} \Big|_{ele} = 4\pi F_e F_e + \frac{1}{2} (D_i D_j F_e)(D^i D^j G_{ele}) \quad (10)$$

$$\frac{1}{\Gamma_{ei}} \frac{\partial F_e}{\partial t} \Big|_{ion} = \frac{4\pi m_e}{m_i} F_e F_i + \frac{M_{cm}}{m_e} (1 - m_e/m_i) (\partial_i F_e)(\partial^i H_{ion}) + \frac{1}{2} (D_i D_j F_e)(D^i D^j G_{ion}) \quad (11)$$

The metric in the (v, θ) coordinate system can be found by transforming the metric of spherical coordinates to obtain

$$g_{ij} = \hat{v}\hat{v} + v^2 \hat{\theta}\hat{\theta} + v^2 \sin^2 \theta \hat{\psi}\hat{\psi} \quad (12)$$

The most complicated term is the tensor formed from the covariant derivative of the velocity-space gradient, which, in terms of ordinary partial derivatives, is

$$D_i D_j F_e = \frac{\partial^2 F_e}{\partial v^i \partial v^j} - \Gamma_{ij}^\lambda \frac{\partial F_e}{\partial v^\lambda} \quad (13)$$

where Γ_{ij}^λ is the affine connection or *Christoffel symbol*¹ and is defined from the metric as

$$\Gamma_{ij}^{\lambda} = \frac{1}{2} g^{\lambda k} \{ \partial_i g_{kj} + \partial_j g_{ki} - \partial_k g_{ij} \} \quad (14)$$

Since F_c is independent of the gyrophase, then only the matrices Γ_{ij}^v and Γ_{ij}^{θ} need be calculated. They are

$$\Gamma_{ij}^v = -v \hat{\rho} \hat{\rho} - v \sin^2 \theta \hat{\phi} \hat{\phi} \quad (15)$$

$$\Gamma_{ij}^{\theta} = \frac{1}{v} \hat{v} \hat{\rho} + \frac{1}{v} \hat{\rho} \hat{v} - \sin \theta \cos \theta \hat{\phi} \hat{\phi} \quad (16)$$

This gives

$$D_i D_j F_c = \begin{pmatrix} \frac{\partial^2 F_c}{\partial v^2} & \frac{\partial^2 F_c}{\partial v \partial \theta} - \frac{1}{v} \frac{\partial F_c}{\partial \theta} & 0 \\ \frac{\partial^2 F_c}{\partial v \partial \theta} - \frac{1}{v} \frac{\partial F_c}{\partial \theta} & \frac{\partial^2 F_c}{\partial \theta^2} + v \frac{\partial F_c}{\partial v} & 0 \\ 0 & 0 & v \sin^2 \theta \frac{\partial F_c}{\partial v} + \sin \theta \cos \theta \frac{\partial F_c}{\partial \theta} \end{pmatrix} \quad (17)$$

and the tensor product of the two double gradients become

$$(1/2) g^{ik} g^{jl} (D_i D_j F_c) (D_k D_l G) = B \frac{\partial F_c}{\partial v} + C \frac{\partial F_c}{\partial \theta} + D \frac{\partial^2 F_c}{\partial v^2} + E \frac{\partial^2 F_c}{\partial \theta^2} + F \frac{\partial^2 F_c}{\partial v \partial \theta} \quad (18)$$

where

$$\begin{aligned} 2B &= \frac{1}{v^3} \left\{ \frac{\partial^2 G}{\partial \theta^2} + 2v \frac{\partial G}{\partial v} + \cot \theta \frac{\partial G}{\partial \theta} \right\} \\ 2C &= \frac{1}{v^3 \sin \theta} \left\{ \frac{2 - \cos^2 \theta}{\sin \theta} \frac{\partial^2 G}{\partial \theta^2} - 2 \sin \theta \frac{\partial^2 G}{\partial v \partial \theta} + \cos \theta \frac{\partial G}{\partial v} \right\} \\ 2D &= \frac{\partial^2 G}{\partial v^2} \\ 2E &= \frac{1}{v^3} \left\{ \frac{\partial^2 G}{\partial \theta^2} + v \frac{\partial G}{\partial v} \right\} \\ 2F &= \frac{2}{v^2} \left\{ \frac{\partial^2 G}{\partial v \partial \theta} - \frac{1}{v} \frac{\partial G}{\partial \theta} \right\} \end{aligned}$$

For the ions, H and G are independent of pitch-angle which allows an analytic expression for the electron-ion collision term and simplifies the tensor term above.

1.3. *The Electron-Ion Term*. Although for electron-electron collisions, the potential, $G_{elec}(v, \theta)$, must be calculated from the evolving electron velocity distribution, the ions are assumed to be Maxwellian. Their potential can be calculated analytically.

Assuming,

$$F_{ion}(v, \theta, \phi) = \frac{n_{ion}}{\pi^{3/2} v_{thi}^3} e^{-(v/v_{thi})^2}$$

where $v_{thi}^2 = T_{ion}/m_i$. Only, the terms $\frac{\partial H_{ion}}{\partial v}$, $\frac{\partial G_{ion}}{\partial v}$, $\frac{\partial^2 G_{ion}}{\partial v^2}$ need be calculated.

$\frac{\partial H_{ion}}{\partial v}$ can be found from Gauss's law and Equation 3,

$$\frac{\partial H_{ion}}{\partial v} = -2 \frac{m_e}{M_{cm}} \frac{n_{ion}}{v_{thi}^2} G(v/v_{thi}) \quad (19)$$

where

$$G(x) = \frac{\text{erf}(x) - (2/\sqrt{\pi})x e^{-x^2}}{2x^2}$$

and, likewise, for G_{ion}

$$\begin{aligned} \frac{\partial G_{ion}}{\partial v} &= \frac{2}{v^2} \frac{M_{cm}}{m_e} \int_0^v H_{ion}(v') v'^2 dv' \\ &= \frac{2}{v^2} \frac{M_{cm}}{m_e} \left\{ \frac{1}{3} v^3 H_{ion}(v) - \frac{1}{3} \int_0^v v'^3 \frac{\partial H_{ion}}{\partial v'} dv' \right\} \end{aligned} \quad (20)$$

But, $H_{ion}(v \rightarrow \infty) \rightarrow 0$, so

$$\begin{aligned} H_{ion}(v) &= - \int_v^\infty \frac{\partial H_{ion}}{\partial v'} dv' \\ &= \frac{m_e}{M_{cm}} \frac{n_{ion}}{v} \text{erf}(v/v_{thi}) \end{aligned} \quad (21)$$

Furthermore,

$$\begin{aligned} \int_0^v v'^3 \frac{\partial H_{ion}}{\partial v'} &= -2 \frac{m_e}{M_{cm}} n_{ion} v_{thi}^2 \int_0^{v/v_{thi}} x^3 G(x) dx \\ &= -\frac{m_e}{2M_{cm}} n_{ion} v^2 \{erf(v/v_{thi}) - 3G(v/v_{thi})\} \end{aligned} \quad (22)$$

which gives

$$\frac{\partial G_{ion}}{\partial v} = n_{ion} \{erf(v/v_{thi}) - G(v/v_{thi})\} \quad (23)$$

and

$$\frac{\partial^2 G_{ion}}{\partial v^2} = \frac{2n_{ion}}{v} G(v/v_{thi}) \quad (24)$$

1.4. Summary of Collision Terms . The Fokker-Plank collision terms can, thus, be summarized as

$$\begin{aligned} \Gamma_e^{-1} \frac{\partial F_e}{\partial t} \Big|_{\text{collisions}} &= (A_{ee} + A_{ei}) F_e + (B_{ee} + B_{ei}) \frac{\partial F_e}{\partial v} + (C_{ee} + C_{ei}) \frac{\partial F_e}{\partial \theta} \\ &\quad + (D_{ee} + D_{ei}) \frac{\partial^2 F_e}{\partial v^2} + (E_{ee} + E_{ei}) \frac{\partial^2 F_e}{\partial \theta^2} + F_{ee} \frac{\partial^2 F_e}{\partial v \partial \theta} \end{aligned} \quad (25)$$

where

$$\begin{aligned} A_{ee} &= 4\pi F_e \\ B_{ee} &= \frac{1}{2v^3} \left\{ \frac{\partial^2 G}{\partial \theta^2} + 2v \frac{\partial G}{\partial v} + \cot \theta \frac{\partial G}{\partial \theta} \right\} \\ C_{ee} &= \frac{1}{2v^3 \sin \theta} \left\{ \frac{2 - \cos^2 \theta}{v \sin \theta} \frac{\partial^2 G}{\partial \theta^2} - 2 \sin \theta \frac{\partial^2 G}{\partial v \partial \theta} + \cos \theta \frac{\partial G}{\partial v} \right\} \\ D_{ee} &= \frac{1}{2} \frac{\partial^2 G}{\partial v^2} \\ E_{ee} &= \frac{1}{2v^4} \left\{ \frac{\partial^2 G}{\partial \theta^2} + v \frac{\partial G}{\partial v} \right\} \\ F_{ee} &= \frac{1}{2v^2} \left\{ \frac{\partial^2 G}{\partial v \partial \theta} - \frac{1}{v} \frac{\partial G}{\partial \theta} \right\} \end{aligned}$$

and

$$\begin{aligned}
 A_{ei} &= 4\pi \frac{m_e}{m_i} F_{ion} \\
 B_{ei} &= \frac{n_{ion}}{v^2} \left\{ \operatorname{erf}(v/v_{thi}) - G(v/v_{thi}) \left[1 + 2(1 - m_e/m_i)(v/v_{thi})^2 \right] \right\} \\
 C_{ei} &= \frac{n_{ion} \cos \theta}{2v^3 \sin \theta} \{ \operatorname{erf}(v/v_{thi}) - G(v/v_{thi}) \} \\
 D_{ei} &= \frac{n_{ion}}{v} G(v/v_{thi}) \\
 E_{ei} &= \frac{n_{ion}}{2v^3} \{ \operatorname{erf}(v/v_{thi}) - G(v/v_{thi}) \}
 \end{aligned}$$

1.5. *A Simple Check* . As a check of the formula, the function $F_e(v, \theta) \sim e^{-(v/v_{the})^2}$ must be a stationary solution to the Fokker-Plank collision operator. Ignoring the slower, electron-ion collisions,

$$\frac{\partial F_e}{\partial t} = 4\pi v_{the}^3 F_e^2 + \frac{n}{x^2} \{ \operatorname{erf}(x) - G(x) \} \frac{\partial F_e}{\partial x} + \frac{n}{x} G(x) \frac{\partial^2 F_e}{\partial x^2} \quad (26)$$

But,

$$\begin{aligned}
 F_e &= \frac{n}{\pi^{3/2} v_{the}^3} e^{-x^2} \\
 \frac{\partial F_e}{\partial x} &= -2xF_e \\
 \frac{\partial^2 F_e}{\partial x^2} &= -2F_e + 4x^2 F_e
 \end{aligned} \quad (27)$$

so that, when Equation 26 is substituted into Equation 25, $\frac{\partial F_e}{\partial t} = 0$. It is also easy to show that when $T_e = T_i$, the electron-ion term vanishes.

2. End Losses .

For particles in the loss-cone, the particle loss rate is given by

$$\left. \frac{\partial F_e}{\partial t} \right|_{\text{losscone}} = -\frac{F_e}{\tau_{\text{transit}}} \quad (28)$$

where $\tau_{transit}$ is the time for a particle to go from the midplane to the mirror-peak.

The loss-boundary is given by $v_{\parallel}(s = s_{mp}) = 0$, or

$$\mu B_{mp} - \frac{q}{m} \Phi_{mp} = \mu B_0 + \frac{1}{2} V_{\parallel,0}^2 - \frac{q}{m} \Phi_0 \quad (29)$$

or

$$V_{\perp,0}^2(1 - R_m) + V_{\parallel,0}^2 = \frac{2q}{m} \Delta\Phi \quad (30)$$

where $\Delta\Phi = \Phi_0 - \Phi_{mp}$, and R_m is the mirror ratio. In (v, θ) phase-space,

$$v^2 \left\{ 1 - R_m \sin^2 \theta \right\} = \frac{2q}{m} \Delta\Phi \quad (31)$$

The condition of being within the loss-region is

$$v^2 > \frac{(2q/m)\Delta\Phi}{1 - R_m \sin^2 \theta} \quad (32)$$

for particles such that $|\sin\theta| < \sqrt{1/R_m}$, and

$$v^2 < \frac{(2q/m)\Delta\Phi}{1 - R_m \sin^2 \theta} \quad (33)$$

for particles such that $|\sin\theta| > \sqrt{1/R_m}$. As can be seen, for positive $\Delta\Phi$, only the first inequality is used, and for negative $\Delta\Phi$, only the second is used.

The transit time is obtained from the equations of motion. Since

$$B(s) = B_0 \left(1 + \frac{s^2}{L^2} \right) \quad (34)$$

$$\Phi(s) = \Delta\Phi \left(1 - \frac{s^2}{L^2} \right) \quad (35)$$

then

$$s(t) = \frac{V_{\parallel,0}}{\omega_{\parallel}} \sin(\omega_{\parallel} t + \psi) \quad (36)$$

where

$$\begin{aligned}\omega_b^2 &= \frac{2}{L^2}(\mu B_0 + (q/m)\Delta\Phi) \\ &= \frac{v^2 \sin^2\theta}{L^2} + \frac{2q\Delta\Phi}{mL^2}\end{aligned}\quad (37)$$

Therefore,

$$\tau_{transit} = \frac{1}{\omega_B} \sin^{-1}\left(\frac{L\omega_B}{v\cos\theta}\right)\quad (38)$$

When $\omega_B < 0$, then $\tau_{transit} \sim \sinh^{-1}(L\omega_B/v\cos\theta)$. Note that Yushmanov particles are not included in this analysis.

Finally, a Maxwellian electron source is often added to the code to maintain the density constant, balancing the loss cone term. When the source temperature is low ($< 10\text{ev}$), this acts to model a cold-plasma stream or an entering flux of secondaries.

3. The ECRH Term .

3.1. *The Diffusion Paths* . The ECRH term used for this code was derived by Mael¹. In this model, only linear heating of trapped, electrons are heated. Since the effect of the heating is bounced-averaged, particles in the loss region of velocity-space are not heated.

The bounce-averaged diffusion equation is

$$\frac{\partial F_e}{\partial t} = \alpha_R^2 \sum_{res} (\rho_{j\omega_c})_{res} \frac{\partial}{\partial \chi} D_{res} \frac{\partial}{\partial \chi} F_e\quad (39)$$

where $\alpha_R^2 = \frac{1}{2} \frac{q^2}{m^2} |E_{rl}|^2$ is the square of the right-handed, electric acceleration, and

$$D_{res} = (\rho_{j\omega_c})_{res} \text{Re}\{\bar{\Omega}_n^{-1}\} J_n^2(\rho k_{\perp})\quad (40)$$

$$\frac{\partial}{\partial \chi} = \frac{1}{B_{res}} \frac{\partial}{\partial \mu} + \frac{\partial}{\partial E}\quad (41)$$

For the program, two diffusion coefficients are defined. These are $D_1 = \sum(\rho_B \omega_c) D_{rcs}$ and $D_2 = \sum(\rho_B \omega_c) \partial D_{rcs} / \partial \chi$, which gives

$$\frac{\partial F_c}{\partial t} = \alpha_r^2 \left\{ D_1 \frac{\partial^2 F_c}{\partial \chi^2} + D_2 \frac{\partial F_c}{\partial \chi} \right\} \quad (42)$$

The gradient along the diffusion path, $\partial / \partial \chi$, can be written in (v, ρ) coordinates by using the identities

$$\begin{aligned} f(E, \mu, v, \theta) &= E - \frac{1}{2} v^2 = 0 \\ g(E, \mu, v, \theta) &= B_0 \mu - \frac{1}{2} v^2 \sin^2 \theta = 0 \end{aligned} \quad (43)$$

and the appropriate Jacobians. For instance,

$$\frac{\partial \theta}{\partial E} = - \frac{\frac{\partial(f, g)}{\partial(E, v)}}{\frac{\partial(f, g)}{\partial(\theta, v)}} = - \frac{\tan^2 \theta}{v^2} \quad (44)$$

and, likewise,

$$\frac{\partial \theta}{\partial \mu} = \frac{B_0}{v^2 \sin \theta \cos \theta} \quad (45)$$

$$\frac{\partial v}{\partial E} = \frac{1}{v} \quad (46)$$

$$\frac{\partial v}{\partial \mu} = 0 \quad (47)$$

This gives the gradient along the diffusion paths as

$$\frac{\partial}{\partial \chi} = \frac{1}{v} \frac{\partial}{\partial v} + \xi \frac{\partial}{\partial \theta} \quad (48)$$

where $\xi = (1/R_{rcs} - \sin^2 \theta) / v^2 \cos \theta \sin \theta$. Also, after some algebra,

$$\frac{\partial^2}{\partial \chi^2} = \frac{1}{v^2} \frac{\partial^2}{\partial v^2} - \frac{1}{v^3} \frac{\partial}{\partial v} + \frac{2\xi}{v} \frac{\partial^2}{\partial \theta \partial v} + \xi^2 \frac{\partial^2}{\partial \theta^2} - \xi \left\{ \xi \frac{2\cos^2\theta - 1}{\sin\theta \cos\theta} + \frac{4}{v^2} \right\} \frac{\partial}{\partial \theta} \quad (49)$$

The ECRH term can then be summarized as

$$\frac{1}{\alpha_R^2} \frac{\partial F_e}{\partial t} \Big|_{ECRH} = B_{ECRH} \frac{\partial F_e}{\partial v} + C_{ECRH} \frac{\partial F_e}{\partial \theta} + D_{ECRH} \frac{\partial^2 F_e}{\partial v^2} + E_{ECRH} \frac{\partial^2 F_e}{\partial \theta^2} + F_{ECRH} \frac{\partial^2 F_e}{\partial v \partial \theta} \quad (50)$$

where

$$\begin{aligned} B_{ECRH} &= \frac{1}{v} D_2 - \frac{1}{v^3} D_1 \\ C_{ECRH} &= \xi \left\{ D_2 - D_1 \left[\xi \frac{2\cos^2\theta - 1}{\sin\theta \cos\theta} + \frac{4}{v^2} \right] \right\} \\ D_{ECRH} &= \frac{1}{v^2} D_1 \\ E_{ECRH} &= \xi^2 D_1 \\ F_{ECRH} &= \frac{2\xi}{v} D_1 \end{aligned}$$

3.2. *The Resonance Function*. In this section, the rules used to evaluate D_{res} are explained. Since $\rho_B k_{\perp} \ll 1$,

$$D_{res} = (\rho_B \omega_c)_{res} \text{Re} \{ \bar{\Omega}_{n=1,2}^{-1} \} \begin{cases} 1, & \text{if } n = 1 \\ (1/4) k_{\perp}^2 \rho_B^2, & \text{if } n = 2 \end{cases} \quad (51)$$

where

$$\text{Re} \{ \bar{\Omega}_n^{-1} \} = \frac{1}{4} \omega_B \tau_{eff}^2 \quad (\text{where } \tau_{eff}^{-2} = \nu'_n / 2) \quad (52)$$

$$\text{Re} \{ \bar{\Omega}_n^{-1} \} = 2\pi \omega_B \tau_{eff}^2 \text{Ai}^2(\nu_n \tau_{eff}) \quad (\text{where } \tau_{eff}^{-3} = \nu''_n / 2) \quad (53)$$

and where $\nu_n = \omega - n\omega_c - k_{\parallel} v_{\parallel}$. Here, all quantities are evaluated at the point of resonance. Equation 51 is used for "simple" resonance points (*ie.* when $\nu_n \rightarrow 0$ while ν' remains finite); and Equation 52 is used for "Airy" resonance points, which occur when both ν_n and $\nu'_n \rightarrow 0$.

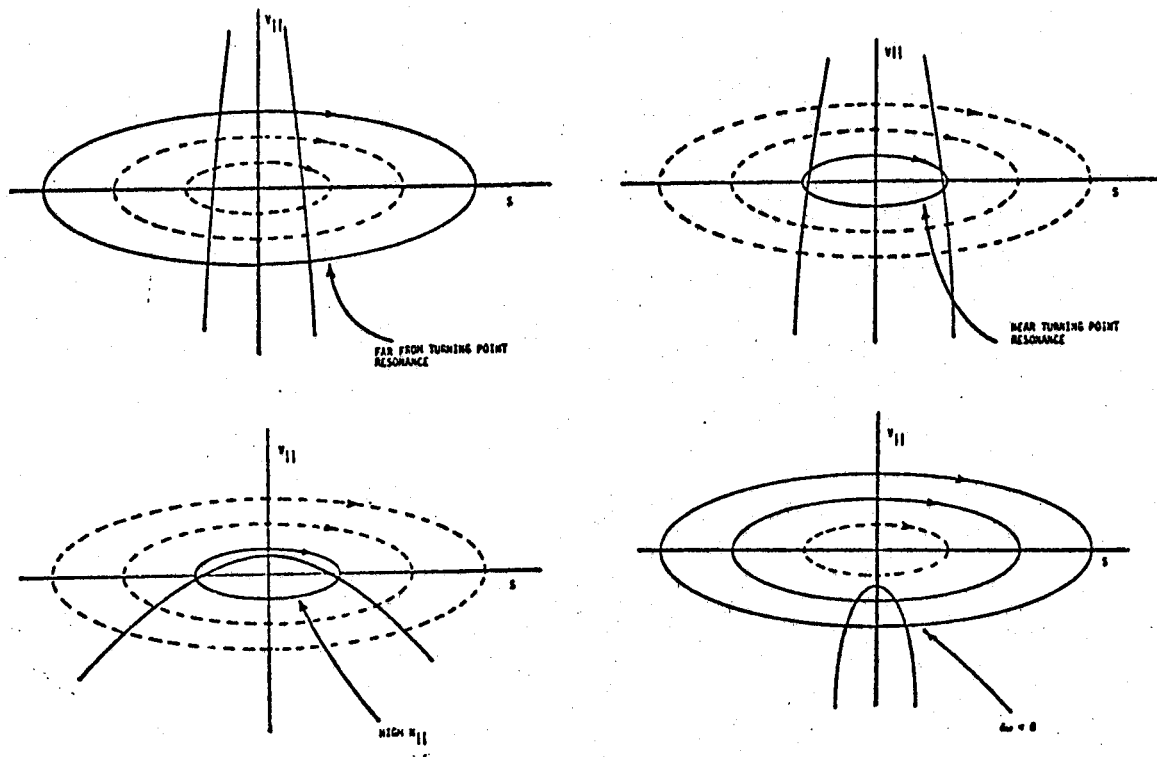


Figure 1. Diagrams of the three classes of bounce-orbits used to determine the sum of the bounce-averaged, resonant wave-particle interactions.

The type and number of resonance points depend upon R_{res} , $k_{||}$, and the actual bounce-orbit of the electron. For the program, these variations can be classified into three categories which are shown in Figure 1. The mirror is assumed to be symmetric for interchange of s with $-s$.

4. Numerical Methods .

The Fokker-Plank equation (Equations 24, 27 and 38) is solved by the modified Alternating Direction Implicit (ADI) method used by Killeen and Marx². A grid in the (v, θ) phase space is defined with variable spacing in the v -direction to provide a wide energy resolution and in the θ -direction to allow quadrature integration. Typically, the grid has 45 v -points and 16- θ points. Integration in the v -direction is performed with Simpson's rule modified to for variable grid spacing².

The ADI solution consists of "splitting" the 2-dimensional partial differential equation into two parts so that the v and θ differences can be taken separately. This gives two equations which can be solved implicitly.

$$\frac{F_e^{t+dt/2} - F_e^t}{\Delta t} = \frac{1}{2}S + \frac{1}{2}AF_e^{t+dt/2} + B\frac{\partial F_e^{t+dt/2}}{\partial v} + D\frac{\partial^2 F_e^{t+dt/2}}{\partial v^2} + \frac{1}{2}F\frac{\partial^2 F_e^{t+dt/2}}{\partial v\partial\theta} \quad (54)$$

$$\frac{F_e^{t+dt} - F_e^{t+dt/2}}{\Delta t} = \frac{1}{2}S + \frac{1}{2}AF_e^{t+dt} + C\frac{\partial F_e^{t+dt}}{\partial\theta} + E\frac{\partial^2 F_e^{t+dt}}{\partial\theta^2} + \frac{1}{2}F\frac{\partial^2 F_e^{t+dt}}{\partial v\partial\theta} \quad (55)$$

If, in each equation, central differences are taken for each derivative (except for a backward derivative for the mixed term), each equation can be written as

$$A^n F_e^{n-1} + B^n F_e^n + C^n F_e^{n+1} = W^n \quad (56)$$

where, for the v -split

$$\begin{aligned} A_v^{n,l} &= \frac{\Delta t}{\Delta v} \left(B - \frac{2D}{\Delta v_-} + \frac{1}{4} \frac{F}{\Delta\theta_-} \right) \\ B_v^{n,l} &= 1 - \frac{1}{2} \Delta t A + \frac{2\Delta t D}{\Delta v} \left(\frac{1}{\Delta v_+} + \frac{1}{\Delta v_-} \right) \\ C_v^{n,l} &= -\frac{\Delta t}{\Delta v} \left(B + \frac{2D}{\Delta v_+} + \frac{1}{4} \frac{F}{\Delta\theta_-} \right) \\ W_v^{n,l} &= F_e^{n,l} + \frac{1}{2} \Delta t S + \frac{\Delta t F}{4\Delta v \Delta\theta_-} (F_e^{n-1,l-1} - F_e^{n+1,l-1}) \\ &\quad + \frac{\Delta t F}{4\Delta v \Delta\theta_+} (F_e^{n+1,l+1} + F_e^{n-1,l-1} - F_e^{n-1,l+1} - F_e^{n+1,l-1}) \end{aligned}$$

and, for the θ -split,

$$\begin{aligned} A_\theta^{n,l} &= \frac{\Delta t}{\Delta\theta} \left(C - \frac{2E}{\Delta\theta_-} + \frac{1}{4} \frac{F}{\Delta v_-} \right) \\ B_\theta^{n,l} &= 1 - \frac{1}{2} \Delta t A + \frac{2\Delta t E}{\Delta\theta} \left(\frac{1}{\Delta\theta_+} + \frac{1}{\Delta\theta_-} \right) \\ C_\theta^{n,l} &= -\frac{\Delta t}{\Delta\theta} \left(C + \frac{2E}{\Delta\theta_+} + \frac{F}{\Delta v_-} \right) \\ W_\theta^{n,l} &= F_e^{n,l} + \frac{1}{2} \Delta t S + \frac{\Delta t F}{4\Delta\theta \Delta v_-} (F_e^{n-1,l-1} - F_e^{n-1,l+1}) \\ &\quad + \frac{\Delta t F}{4\Delta\theta \Delta v_+} (F_e^{n+1,l+1} + F_e^{n-1,l-1} - F_e^{n+1,l-1} - F_e^{n-1,l+1}) \end{aligned}$$

where

The boundary conditions of the program are

$$1. \left. \frac{\partial F_e}{\partial v} \right|_{v=0, \theta=\pi/2} = 0 \text{ due to azimuthal symmetry. } F_e^{0,1} = F_e^{1,1}.$$

$$2. F_e(n = N) = 0.$$

$$3. F_e^{0,l} \text{ is independent of } l \text{ (ie } \theta).$$

$$4. \left. \frac{\partial F_e}{\partial \theta} \right|_{\theta=0, \pi} = 0 \text{ due to azimuthal symmetry. } F_e^{n,L-1} = F_e^{n,L}.$$

$$5. \left. \frac{\partial F_e}{\partial \theta} \right|_{\theta=\pi/2} = 0 \text{ from bounce-direction symmetry.}$$

These boundary conditions are used to combine or eliminate terms in the upper left and bottom right corners of the matrix. In this way, the initial conditions for the sweep out and back through the grid indices are determined.

Finally, note that all of the gradients of $G_{elc}(v, \theta)$ needed for the electron-electron collision term can be found using central differences since all of the boundary points are obtained implicitly from the interior points and the boundary conditions.

5. Diagnostics .

The following diagnostics are available to analyze the program's results during simulation of ECRH of Constance 2: 1. $F_e(v, \theta)$, 2. $F_e(E)$ and $F_e(\theta)$, 3. $\langle E \rangle(t)$, 4. $n_e(t)$, 5. $I_{oss,e}(t)$, and 6. $I_{oss,e}(E)$.

6. Examples and Checks .

Figure 2 shows an example of the relaxation of a non-Maxwellian electron population due to electron-electron collisions. Four contour plots of $(V_{\perp}, V_{\parallel})$ phase-space are shown for $t = 0, 5, 10,$ and $20 \mu\text{sec}$. The energy and density were constant to within 0.5%.

Figure 3 gives an example of the change in the average electron energy and total endloss when ECRH is applied. The ECRH parameters were $N_{\parallel} = 2.0$, $|E_r| = 10 \text{ v/cm}$, and $R_{res} = 1.06$. The density was fixed at $2.0 \times 10^{12} \text{ cm}^{-3}$, the potential fixed at 25 V , $T_{ion} = 170 \text{ ev}$, $R_b = 2$, and a cold electron source ($T_{src} = 10 \text{ ev}$) was added with a current equal to one-tenth the the total loss current. Figure 4 shows the development of the electron energy distribution, and Figure 5 gives four examples of the resulting

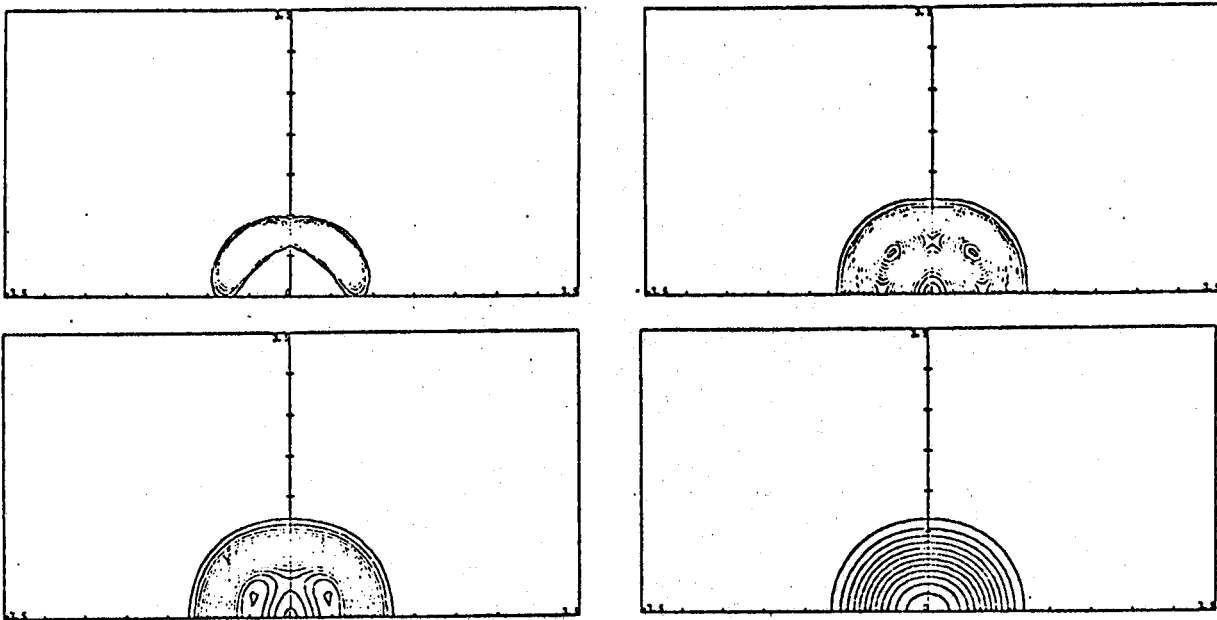


Figure 2. The development of the electron distribution for a relaxing non-Maxwellian distribution due to electron-electron collisions. $n_e = 2.0 \times 10^{12} \text{cm}^{-3}$, and $T_e = 255 \text{eV}$. The density and energy remained constant to within 0.5%. 20 equally-spaced contours were drawn for each plot.

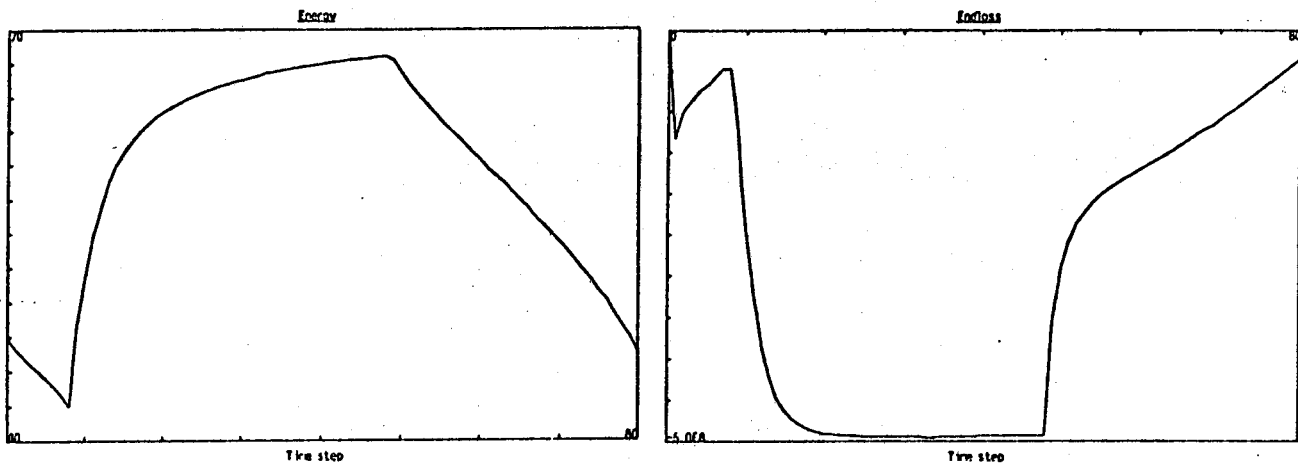


Figure 3. The change of the average electron energy and the total endloss with time. The run lasted $20 \mu\text{sec}$ with the ECRH $10 \mu\text{sec}$ long. Many features of the run are similar to those observed in the experiment, such as the enhanced endlosses, the "ECRH equilibrium", the non-maxwellian energy distribution, and the energy distribution of the endloss.

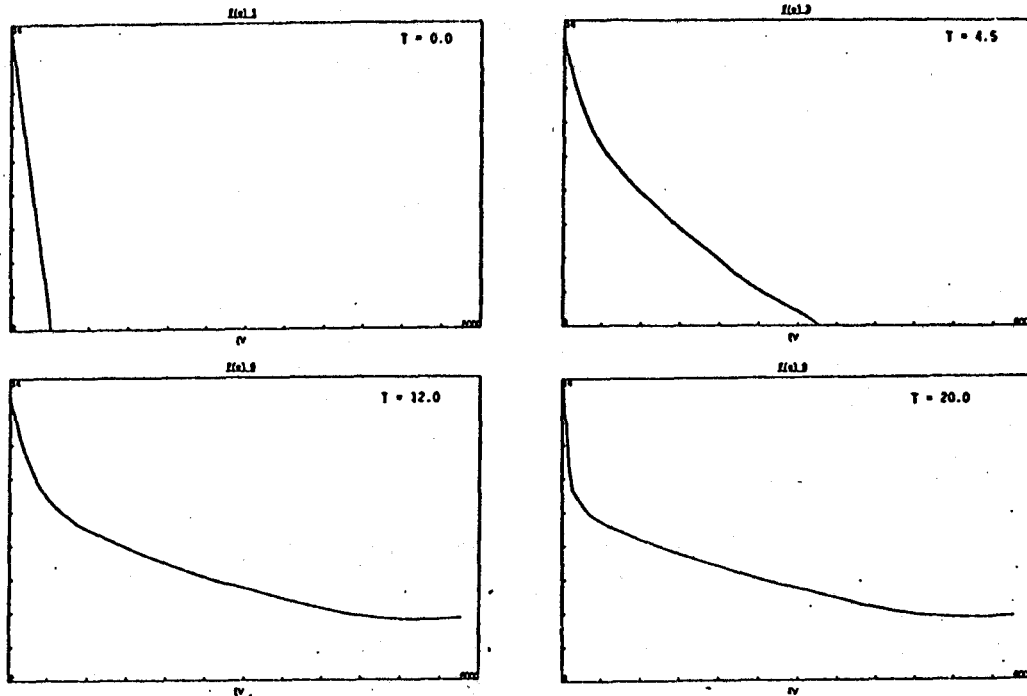


Figure 4. The change in the electron energy distribution due to ECRH. $\omega/\omega_{c0} = 1.06$, $|E_r| = 10.0V/cm$, and $N_{||} = 2.0$. For $t = 0, 4.5, 12,$ and $20 \mu sec$.

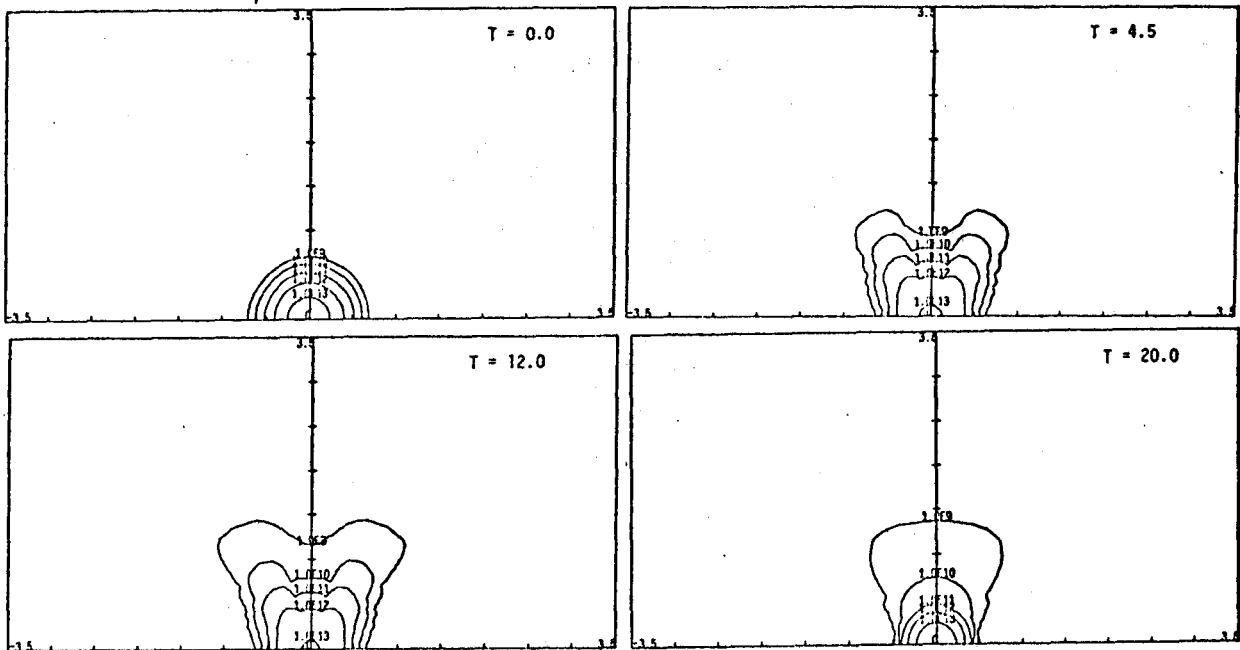


Figure 5. The electron phase-space corresponding to the four times shown in Figure 4.

velocity-space distribution as the run progressed. Many features of the run are similar to those observed in the experiment, such as the enhanced endlosses, the "ECRH equilibrium", the non-maxwellian energy distribution, and the energy distribution of the endloss.

References

1. Mauel, M. E., *Theory of Electron Cyclotron Heating in the Constance II Experiment*, PFC-RR-81/2, Massachusetts Institute of Technology, (1981).
2. Killeen, J. and K. D. Marx, "The solution of the Fokker-Plank Equation for a Mirror-Confined Plasma," *Advances in Plasma Physics*, Vol. 7, (1977), 421-489.
3. Cutler, T. A., L. D. Pearlstein and M. E. Rensink, *Computation of the Bounce-Average Code*, UCRL-52233, LLL, (1977).
4. Rosenbluth, M. N., W. M. MacDonald, and D. L. Judd, "Fokker-Plank Equation for an inverse-Square Force.," *Physical Review*. 107, (1957), 1-6.
5. Weinberg, S., *Gravitation and Cosmology*, Wiley, New York, (1972), 91-120.
6. Hornbeck, R. W., *Numerical Methods*, Quantum, New York, (1975).

PFC BASE LIST

INTERNAL MAILINGS (MIT)

G. Bekefi
36-213

A. Bers
38-260

D. Cohn
NW16-250

B. Coppi
26-201

R.C. Davidson
NW16-202

T. Dupree
38-172

S. Foner
NW14-3117

J. Freidberg
38-160

A. Gondhalekar
NW16-278

M.O. Hoenig
NW16-176

M. Kazimi
NW12-209

L. Lidsky
38-174

E. Marmar
NW16-280

J. McCune
31-265

J. Meyer
24-208

D.B. Montgomery
NW16-140

J. Moses
NE43-514

D. Pappas
NW16-272

R.R. Parker
NW16-288

N.T. Pierce
NW16-186

P. Politzer
NW16-286

M. Porkolab
36-293

R. Post
NW21-

H. Praddaude
NW14-3101

D. Rose
24-210

J.C. Rose
NW16-189

R.M. Rose
4-132

B.B. Schwartz
NW14-5121

R.F. Post
NW21-203

L.D. Smullin
38-294

R. Temkin
NW16-254

N. Todreas
NW13-202

J.E.C. Williams
NW14-3210

P. Wolff
36-419

T.-F. Yang
NW16-164

Industrial Liaison Office
ATTN: Susan Shansky
Monthly List of Publications
39-513

MIT Libraries
Collection Development
ATTN: MIT Reports
14E-210

B. Colby
PFC Library
NW16-255

EXTERNAL MAILINGS

National

Argonne National Laboratory
Argonne, IL 60439
ATTN: Library Services Dept.

Dr. D. Overskei
General Atomic Co.
P.O. Box 81608
San Diego, CA 92138

Battelle-Pacific Northwest Laboratory
P.O. Box 99
Richland, WA 99352
ATTN: Technical Information Center

Princeton Plasma Physics Laboratory
Princeton University
P.O. Box 451
Princeton, NJ 08540
ATTN: Library

Brookhaven National Laboratory
Upton, NY 11973
ATTN: Research Library

Plasma Dynamics Laboratory
Jonsson Engineering Center
Rensselaer Polytechnic Institute
Troy, NY 12181
ATTN: Ms. R. Reep

U.S. Dept. of Energy
Washington, D.C. 20545
ATTN: D.O.E. Library

University of Wisconsin
Nuclear Engineering Dept.
1500 Johnson Drive
Madison, WI 53706
ATTN: UV Fusion Library

Roger Derby
Oak Ridge National Lab.
ETF Design Center
Bldg. 9204-1
Oak Ridge, TN 37830

General Atomic Co.
P.O. Box 81608
San Diego, CA 92138
ATTN: Library

Lawrence Berkeley Laboratory
1 Cyclotron Rd.
Berkeley, CA 94720
ATTN: Library

Lawrence Livermore Laboratory
UCLA
P.O. Box 808
Livermore, CA 94550

Oak Ridge National Laboratory
Fusion Energy Div. Library
Bldg. 9201-2, ms/5
P.O. Box "Y"
Oak Ridge, TN 37830

EXTERNAL MAILINGS

International

Professor M.H. Brennan
Willis Plasma Physics Dept.
School of Physics
University of Sydney
N.S.W. 2006, Australia

Division of Plasma Physics
Institute of Theoretical Physics
University of Innsbruck
A-6020 Innsbruck
Austria

c/o Physics Section
International Atomic Energy Agency
Wagramerstrasse 5
P.O. Box 100
A-1400 Vienna, Austria

Laboratoire de Physique des Plasmas
c/o H.W.H. Van Andel
Dept. de Physique
Universite de Montreal
C.P. 6128
Montreal, Que H3C 3J7
Canada

Plasma Physics Laboratory
Dept. of Physics
University of Saskatchewan
Saskatoon, Sask., Canada S7N 0W0

The Library
Institute of Physics
Chinese Academy of Sciences
Beijing, China

Mrs. A. Wolff-Degives
Kernforschungsanlage Julich GmbH
Zentralbibliothek - Exchange Section
D-5170 Julich - Postfach 1913
Federal Republic of Germany

Preprint Library
Central Research Institute for Physics
H-1525 Budapest, P.O. Box 49
Hungary

Plasma Physics Dept.
Israel Atomic Energy Commission
Soreq Nuclear Research Center
Yavne 70600
Israel

The Librarian (Miss DePalo)
Associazione EURATOM - CNEN Fusione
C.P. 65-00044 Frascati (Rome)
Italy

Librarian
Research Information Center
Institute of Plasma Physics
Nagoya University
Nagoya, 464
Japan

Dr. A.J. Hazen
South African Atomic Energy Board
Private Bag X256
Pretoria 0001
South Africa